Electronic and mechanical properties of C_{60}-doped nanotubes

2001 J. Phys.: Condens. Matter 13 8049

(http://iopscience.iop.org/0953-8984/13/35/312)

INSTITUTE OF PHYSICS PUBLISHING JOURNAL OF PHYSICS: CONDENSED MATTER

J. Phys.: Condens. Matter **13** (2001) 8049–8059 PII: S0953-8984(01)22176-6

Electronic and mechanical properties of C_{60}-doped nanotubes

Amir A Farajian[1] **and Masuhiro Mikami**

Research Institute for Computational Sciences, National Institute of Advanced Industrial Science and Technology, Tsukuba 305-8568, Japan

E-mail: amir@imr.edu (A A Farajian)

Received 20 February 2001
Published 16 August 2001
Online at stacks.iop.org/JPhysCM/13/8049

Abstract

Using a generalized tight-binding model, we study the changes induced in the electronic and mechanical properties of carbon nanotubes with encapsulated C_{60}s. Provided enough overlap exists between the electronic states of the nanotube and those of the C_{60}s, a tiny gap (∼0.01–0.02 eV) opens in the band structure of a metallic tube. The gap is seen to be wider for smaller separations between the C_{60}s. For semiconductor tubes, on the other hand, the encapsulated C_{60}s produce donor levels in the gap causing it to narrow. As regards mechanical properties, doped tubes are observed to be slightly 'softer' than undoped ones. This is indicated by reductions of the Young modulus and torsional rigidity of the doped tubes by 0.4–1.8% and 0.6–1.2%, respectively, as compared to those of the pure tubes. Moreover, the Poisson ratio of the doped tubes is seen to be lower by ∼5%. These novel features of the fullerene-doped nanotubes should be of interest in future applications.

1. Introduction

The experimental observation of single-wall carbon nanotubes encapsulating fullerene cages [1–4] gives rise to the natural question of to what extent the electronic and mechanical properties of the fullerene-doped nanotubes would be altered as a result of doping. In experiments, the encapsulated cages, the majority of which were reportedly C_{60}s, were positioned in such a way that a preferred van der Waals separation (0.3 nm) was maintained between the cages and the nanotubes. It was suggested [3] that the presence or absence of encapsulated cages was strongly correlated with the tubes' diameters, mostly observed to be 1.3–1.4 nm. In a row of encapsulated C_{60}s concentric with a tube axis, the centre-to-centre distance between two C_{60}s was observed to be 1.0 nm [1], whereas for paired C_{60}s, this distance

[1] Present address: Institute for Materials Research, Tohoku University, Sendai 980-8577, Japan.

was 0.9 nm [3]. These distances agree with the C_{60} separations in face-centred-cubic and dimer structures, respectively.

The relatively large separation between the encapsulated C_{60}s and the nanotubes observed in experiments makes the overlap and hybridization of electronic states less likely. Therefore one does not expect the encapsulation of C_{60}s to significantly alter the electronic structure of the nanotubes which are 1.3–1.4 nm in diameter. From a theoretical point of view, however, it is possible to investigate changes in electronic structure of doped nanotubes when there is stronger overlap of electronic states, e.g., for tubes with smaller radii. The van der Waals interaction between the C_{60}s and the nanotube, on the other hand, is strong enough to induce slight changes in mechanical properties of the nanotube.

Here, we study the electronic and mechanical properties of C_{60}-doped single-wall carbon nanotubes, focusing on the differences between doped and pure materials. Calculating total energies, we first concentrate on the favoured positions of the C_{60}s within the nanotube. Next, the electronic structures of several doped nanotubes are derived and compared with the undoped cases. Finally we consider mechanical characteristics, calculate the Young modulus and torsional rigidity of the doped tubes, and investigate the changes in Poisson ratio as a result of doping.

2. Model and method

The main system considered here in making the total-energy and relaxation calculations includes a (10, 10) tube, whose diameter is 13.6 Å. This particular nanotube is special among armchair tubes as it is of precisely the right size to accommodate a C_{60} inside it with the appropriate van der Waals spacing [5]. Moreover, as the armchair tubes are energetically more stable [6], the choice of an armchair tube among tubes having almost the same diameter is appropriate. It should be mentioned, however, that the effect of chirality on the elastic properties is small [6]. For the calculations of the electronic structure and density of states (DOS), on the other hand, several different tubes are considered. These include tubes of different chiralities/diameters which will be introduced later. A supercell in our calculation will therefore contain part of a nanotube encapsulating a few C_{60}s. The exact length of the tube within the supercell as well as the number of encapsulated C_{60}s are subject to change according to the specific case under consideration.

In order to model the system, we use a tight-binding formalism with the Xu *et al* parametrization for carbon [7], which has proven to be a transferable potential in tight-binding studies of carbon systems. This parametrization, however, is insensitive to the van der Waals interactions, which should be taken care of separately. The van der Waals interaction is shown to be important in explaining the experimental results on fullerene systems in which the interactions of separate carbon clusters play a crucial role. These include, e.g., phase transitions in solid C_{60} [8] as well as Raman spectra [9] and vibrational modes [10] of nanotube bundles. In these studies, the experimental results were reproduced, with satisfying accuracy, by summing over all interfullerene carbon–carbon interactions using a Lennard-Jones potential. The same Lennard-Jones model was also used to study the shape of large multiple-shell fullerenes [11]. Here, we use the same Lennard-Jones pair potential, i.e.,

$$U(r) = 4\varepsilon[(\sigma/r)^{12} - (\sigma/r)^{6}]$$

with $\varepsilon = 2.964$ meV and $\sigma = 3.407$ Å, in order to include the interfullerene van der Waals interactions. The cut-off radius used to determine which atoms are neighbours is set at 5.5 Å. For each atom in a basal plane of graphite, for example, this corresponds to including the interactions of up to six nearest neighbours in the adjacent layers.

As the number of carbon atoms in the system under study is rather large (typically 680–1020), it is important to use efficient methods for total-energy/relaxation calculations. Therefore the O(N) density-matrix electronic structure calculation method proposed by Li *et al* [12] is used in the present study. This method is based upon a variational solution for the density matrix, and has proven to be faster than the conventional methods of electronic structure calculation for large systems. As for the structure relaxation, which is crucial, especially in calculating mechanical properties such as the Young modulus and torsional rigidity, we use the Broyden minimization scheme [13]. Using this method, it is practical to reach force accuracies[2] of better than 1 meV Å^{-1} with moderate computational effort. This convergence criterion is imposed on all the calculations involving structure relaxation here, unless otherwise specified.

For obtaining the electronic structure and DOS, we use direct diagonalization with 1000 k-points to calculate the band structure. This reveals the fine changes, e.g., tiny gaps, introduced into the band structure as a result of doping. The DOS curves are then obtained by broadening each eigenvalue with a Gaussian of 0.005 eV width.

As a reliability test for the present approach, we checked that the calculated interlayer separation and Young modulus along the c-axis of a relaxed slab of graphite, made up of nine sheets of carbon atoms, were indeed in excellent agreement with the experimental results. This was anticipated, however, as the relevant van der Waals parameters were originally fitted [8] to reproduce the experimental results. As a non-trivial test, we also calculated the elastic constant c_{44} of the same graphite slab. It is observed that infinitesimal (up to 0.5 Å) changes in the positions of atoms in a basal plane result in modifications of atomic positions in the four nearest planes. A second-order polynomial fit to the resulting energy curves determines the second derivative to be 0.224 eV/atom. Taking the effective thickness of a graphite sheet to be 3.4 Å, the elastic constant c_{44} is estimated to be 0.004 TPa. This agrees excellently with the experimental result ($\geqslant$0.004 TPa) reported by Seldin and Nezbeda [14].

In addition to the above tests for graphite, we also compared the Young moduli of single- and double-wall tubes with diameter 13.6 Å, calculated using the present model, against the *ab initio* results of Sánchez-Portal *et al* [6]. As will be shown shortly, the agreement is very good. It should be mentioned that throughout this paper whenever the Young modulus is converted from eV/atom (for the second derivative of energy with respect to the axial strain) to TPa, the above-mentioned effective thickness is assumed for the nanotube wall(s).

3. Results and discussion

3.1. Preferred positions of C_{60} molecules

In order to obtain the favoured positions of the C_{60}s inside the nanotube, we perform two different sets of calculations. First, a portion of the (10, 10) tube containing 600 atoms, and 36.37 Å in length, is considered in the supercell. A C_{60} is then located inside the tube, and several total-energy calculations are performed for different distances between the C_{60} centre and the nanotube axis. At each distance, the energy calculation is performed after fully relaxing the structure, as discussed earlier. In these relaxations the separation of the C_{60} and the nanotube is fixed. This is achieved by fixing the atoms belonging to two of the C_{60} hexagons, which are almost perpendicular to the radial direction passing through the centre of the C_{60}. These two hexagons are therefore the closest and furthest ones with respect to the nanotube axis. Moreover, two rings, of 20 carbon atoms each, at each end of the nanotube are also fixed

[2] Total-energy convergence turns out not to be sufficient in structure relaxations, as a high degree of energy convergence does not necessarily mean a high degree of convergence for all the force components, but the reverse is always true.

throughout the relaxations discussed here, as well as all other relaxations to be discussed later. This is done in order to prevent distortions at the open ends of the nanotubes, as we do not impose periodic boundary conditions on the nanotubes in calculations involving relaxation.

The results of total-energy calculations for different distances between the C_{60} centre and the nanotube axis, shown in figure 1(a), indicate that the favoured position of the C_{60} along the radial direction of the nanotube occurs when the C_{60} centre coincides with the nanotube axis. This is mainly due to the van der Waals repulsion, as the cut-off of the tight-binding model that we use here is 2.6 Å. Therefore, from now on, we will assume that all the encapsulated C_{60}s are concentric with the nanotube axis.

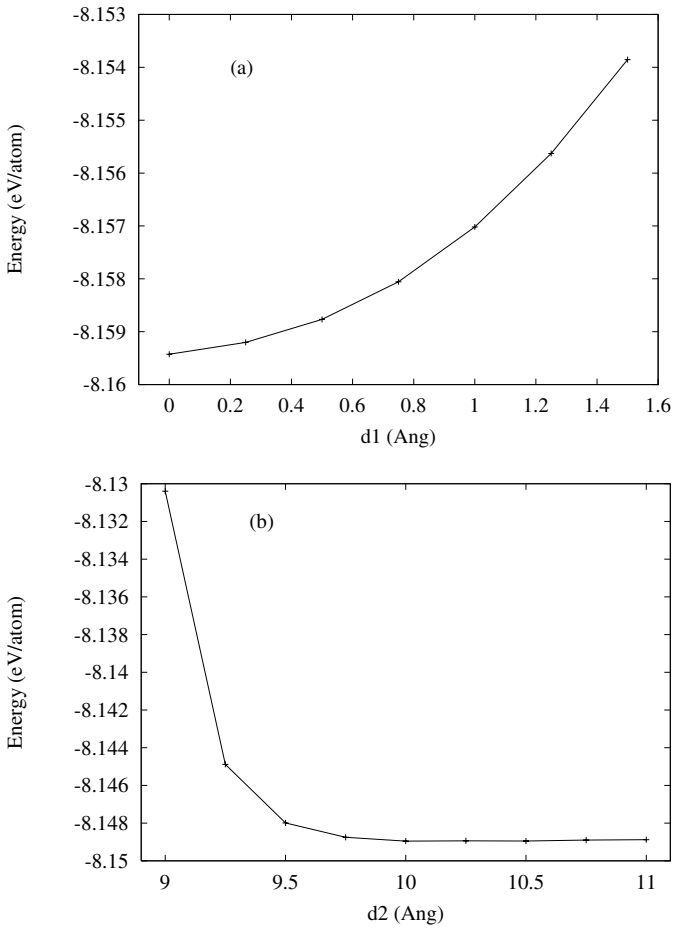

Figure 1. (a) Total energy for relaxed structures at different values of the distance between the C_{60} centre and the nanotube axis, d1. (b) Total energy for different values of the distance between the centres of neighbouring C_{60}s, d2.

A second set of calculations is next performed to derive the total energy of the system as a function of the distance between the centres of different C_{60}s. To this end, we put two C_{60}s inside the same nanotube portion as described above, and calculate the total energy of the relaxed structures for different separations of those two C_{60}s. Here, the inter-C_{60} distance (the distance between the centre of neighbouring C_{60}s) is kept fixed during the relaxation by fixing four carbon atoms in each C_{60}, which are the closest atoms with respect to the other

one. Figure 1(b) depicts the results thus obtained. Despite the sharp increase in the repulsion force for distances less than 9.5 Å, the energy curve is observed to be essentially flat for distances greater than 10 Å. (It should be mentioned that here we concentrate on the range of distances possible without the formation of a chemical bond between the C_{60}s.) Although no significant minimum is found at large separations, the presence of other C_{60}s would sandwich each C_{60} between its two neighbours at a favoured distance of ∼10–10.5 Å due to van der Waals repulsion. The ending C_{60}s of a chain would then be kept in place by, e.g., caps of the nanotube or distortions in its wall. This latter case, however, might not result in a completely stable configuration, and activated 'jumps' of the C_{60}s would be possible. Examples of these jumps have in fact been reported by Smith *et al* [3].

3.2. Electronic properties

As described before, for tubes with diameters in the experimentally observed range 1.3–1.4 nm, one does not expect significant changes in electronic properties induced by encapsulated C_{60}s, due to the relatively large separation of the electronic states. In fact, the tight-binding model considered here is insensitive to the overlap of the states whose corresponding atoms are separated by more than 2.6 Å. Therefore, within the formalism adopted here, the DOS curves corresponding to (10, 10) and (17, 0) tubes doped with C_{60}s would be a mere superposition of the pure-tube DOS and the C_{60}-chain DOS, and there would be no overlap of electronic states. The above-mentioned tubes, i.e., (10, 10) and (17, 0), are metallic and semiconductor tubes, respectively, whose diameters lie within the experimentally observed range. In order to enhance the overlaps and to make the electronic structure changes of the doped tubes detectable within the present tight-binding formalism, we therefore choose two other tubes with smaller radii. These are a metallic (8, 8) tube and a semiconductor (14, 0) tube, whose diameters are 10.7 and 10.8 Å, respectively. Although these tubes are not experimentally observed to encapsulate C_{60}s, one can assume the changes induced in the electronic structure of these tubes to be somewhat enhanced versions of the corresponding changes for larger tubes. In other words, it is reasonable to expect the results obtained for the (8, 8) and (14, 0) tubes to qualitatively hold for the (10, 10) and (17, 0) tubes with minor modifications.

We first consider the case of the doped (14, 0) tube. A portion of this tube, with a length of 8.4 Å, is considered in the unit cell. It is assumed that this portion encapsulates one C_{60}. This would make the inter-C_{60} distance the same as the unit-cell length, i.e., 8.4 Å, which is compatible with the inter-C_{60} distance in the C_{60} dimer [15]. The results of the DOS calculation for both the doped tube and the pure one are shown in figure 2(a). It is clear that the encapsulated C_{60}s act as donor impurities for the semiconductor (14, 0) nanotube, as there are (empty) donor levels produced within the gap as a result of doping. This causes a narrower gap which can be more easily closed due to, e.g., lattice vibrations. The fact that C_{60}s have the same effect as donor impurities makes the fullerene-doped semiconductor nanotubes suitable for transport applications, e.g., nano-diodes [16, 17], in which doping is required to modify the electronic structure of part of the nanotube.

Next, the electronic structure of the doped (8, 8) tube is calculated. In this case we distinguish between two different situations: (i) the inter-C_{60} distance equal to 9.7 Å; and (ii) the inter-C_{60} distance equal to 8.49 Å. The calculated DOS of the pure tube together with those of the cases (i) and (ii) are depicted in figure 2(b). The hybridization of the electronic states of the tube with those of the C_{60}s is seen to produce several levels within the pseudo-gap of the metallic tube. Although the DOS curves, obtained by broadening each eigenvalue with a Gaussian of 0.005 eV width, reveal the production of tiny gaps at the Fermi level, the structure of the gaps can be better observed using the band structures. Therefore in figure 3 we show the

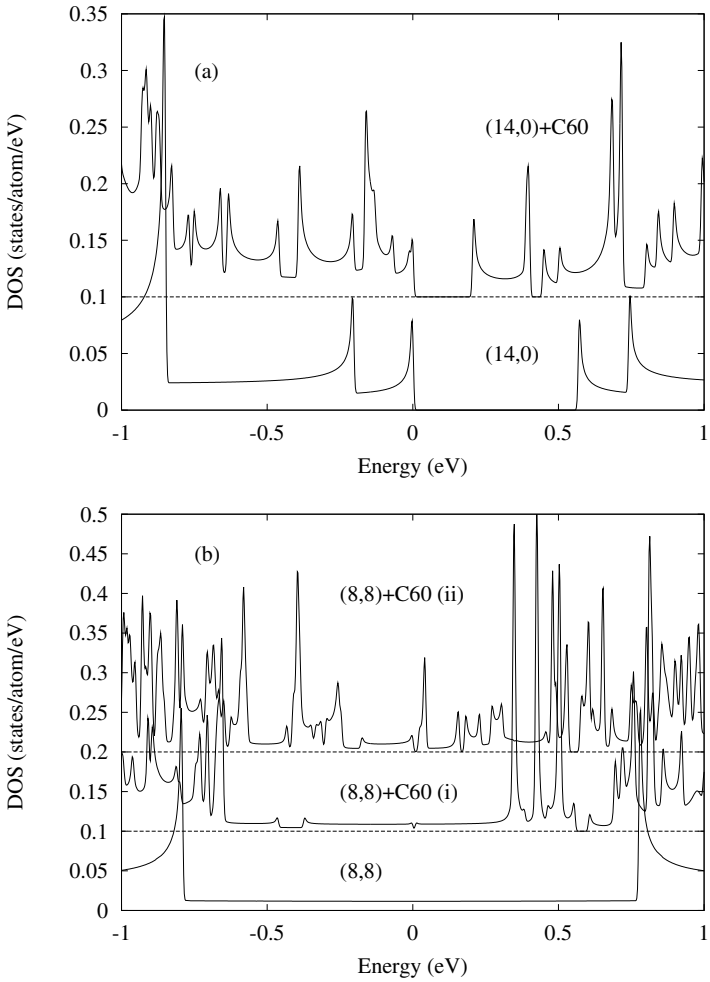

Figure 2. (a) Densities of states (DOS) for the pure and doped (14, 0) tubes. For clarity, the DOS curve of the doped (14, 0) tube is shifted vertically by 0.1. (b) DOS curves for the pure and doped (8, 8) tubes. Cases (i) and (ii) refer to two inter-C_{60} distances. For clarity, the DOS curves of the cases (i) and (ii) are shifted vertically by 0.1 and 0.2, respectively. The top of the valence band, for all curves, is shifted to zero.

highest occupied and the lowest unoccupied levels. From this figure it is clear that a tiny gap opens as a result of doping. The width of this gap is sensitive to the inter-C_{60} separation: the gap corresponding to case (ii) is twice that corresponding to case (i). Although the gap width is rather small, it nevertheless indicates a tendency towards metal-to-semiconductor transition in an all-carbon system, which is an interesting feature of the fullerene-doped metallic nanotubes. This feature is reminiscent of a similar gap-opening observed in metallic nanotube bundles [18].

3.3. Young modulus and torsional rigidity

One might be inclined to think that the fullerene-doped nanotubes are 'stiffer', i.e., show more resistance to contraction/elongation as well as torsion, as compared to the pure tubes. This idea arises from modelling the nanotube and the encapsulated C_{60} chain, each with an effective set

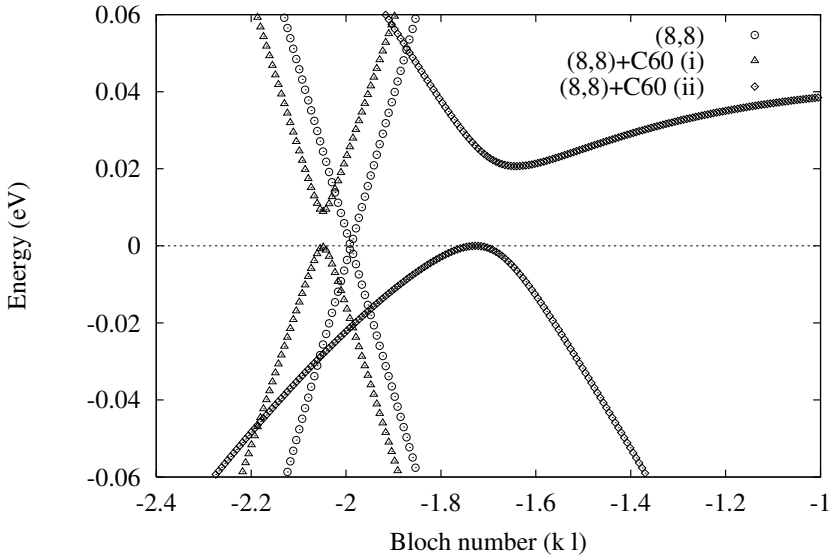

Figure 3. The highest filled and lowest empty levels for the pure and doped (8, 8) tubes. Cases (i) and (ii) refer to two inter-C_{60} distances. The tops of the valence bands are shifted to zero.

of springs, and considering these two sets to be connected *in parallel*. Here we show, however, that this is not the case, at least for the non-dimerized C_{60} chains where the centre-to-centre distance of the neighbouring C_{60}s lies within ∼10–10.5 Å. In fact, the doped nanotubes are observed to be slightly 'softer' under contraction/elongation/torsion. Using the spring analogy described above, the van der Waals interaction between the C_{60}s on one hand and the nanotube on the other causes the effective springs corresponding to the nanotube to be connected *in series* with the effective springs of the C_{60} chain.

In order to calculate the Young modulus and torsional rigidity of the doped tubes, we consider a portion of the (10, 10) nanotube whose length is 41.22 Å, with the initial C–C bond lengths of 1.4 Å. The portion contains four C_{60}s, with the inter-C_{60} separation initially set to 10.5 Å. Constrained relaxation is performed for different amounts of contraction/elongation as well as torsion, in order to obtain the optimized geometries and the corresponding total energies. Throughout the constrained relaxations, two carbon rings at each end of the nanotube, together with the four outermost carbon atoms in each of the ending C_{60}s, are kept fixed in order to fix the axial strain/torsion angle. The total-energy results for both the doped and pure materials are shown in figure 4. In addition, in this figure the results for the double-wall nanotube (10, 10) + (5, 5) are given for comparison.

Upon fitting the data depicted in figures 4(a) and 4(b) with second-order polynomials, one can obtain the Young modulus and torsional rigidity through the relations [19] $F = \frac{1}{2}Eu_{zz}^2$ and $F = \frac{1}{2}c\tau^2$, respectively. Here, F is the Helmholtz free energy (for which we use the total energy of the relaxed structure), E is the Young modulus, u_{zz} is the axial strain, and c and τ are the torsional rigidity and torsion angle per unit length, respectively. We obtain the Young moduli of the pure and double-wall tubes as 52.47 eV/atom and 51.86 eV/atom (=0.94 TPa), respectively. These values agree excellently with the results of *ab initio* calculations (52 eV/atom and 0.92 TPa, respectively) reported by Sánchez-Portal *et al* [6]. As for the torsional rigidity, the corresponding values for the pure and double-wall tubes are obtained as 0.25 and 0.19 eV Å^2 deg^{-2}/atom, respectively.

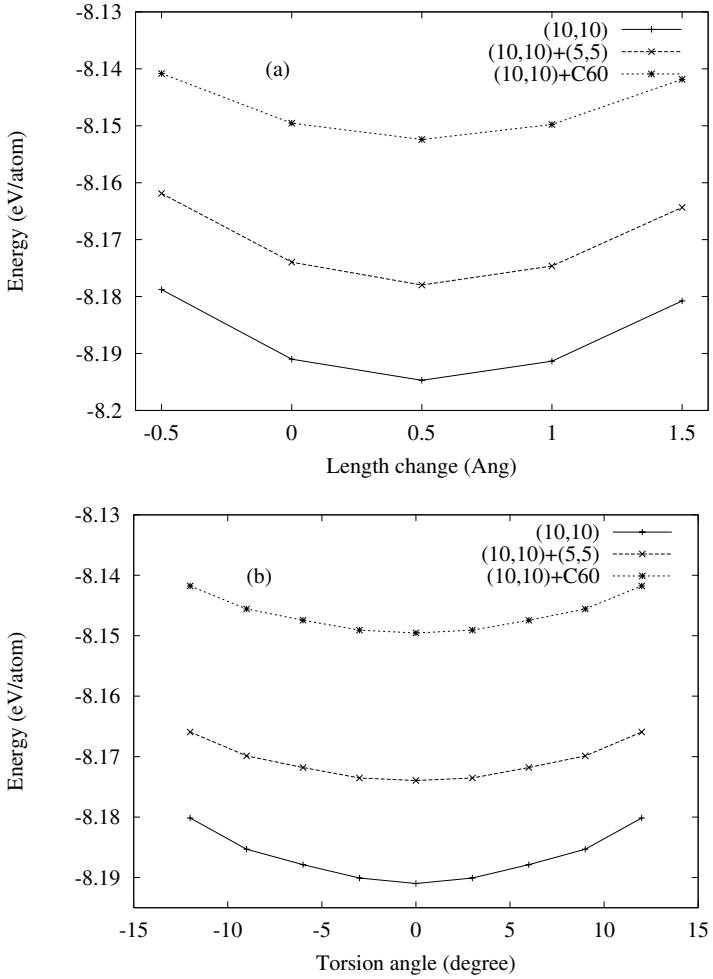

Figure 4. Total energy per atom for pure and doped (10, 10) nanotubes for different length changes (a) and torsion angles (b).

The case of the C_{60}-doped tubes is, however, somewhat tricky. This is because of the fact that, unlike the case for the pure tube, the stress/torsion energy is not evenly distributed among all the atoms in the C_{60} + nanotube system, due to the weak van der Waals coupling between the C_{60}s and the tube. Therefore, using the definitions of the Young modulus and torsional rigidity based upon energy per atom—henceforth referred to as the conventional definitions—would be misleading, as they include the total volume of the system. In fact, using the conventional definitions, one would get *much* (up to ∼30%) lower values for the Young modulus and torsional rigidity of the C_{60}-doped tubes as compared to the pure ones, simply because of the unrealistic assumption of evenly distributed stress/torsion energy. As measures for the Young modulus and torsional rigidity better suited for the present case, we propose[3] the use of E_L and c_L, defined by $F_L = \frac{1}{2}E_L u_{zz}^2$ and $F_L = \frac{1}{2}c_L\tau^2$, respectively. Here, F_L is the total energy per unit length of the system at equilibrium: $F_L = F/L_0$, with L_0 being the length at zero stress. For any given inter-C_{60} distance, the equilibrium length L_0

[3] Compare with a similar proposal of using total energy per unit surface in calculating the Young modulus; see [20].

of the system has a well-defined value. Therefore, E_L and c_L, as defined above, provide us with sensible measures for comparing the Young modulus and torsional rigidity of pure and doped nanotubes.

Using the data of figure 4 multiplied by the corresponding number of atoms and divided by the equilibrium length, the values of E_L for the pure, C_{60}-doped, and double-wall nanotubes are obtained as 854.85, 851.59, and 1266.95 eV Å^{-1}, respectively. Similarly, the values of c_L for the pure, C_{60}-doped, and double-wall nanotubes are obtained as 4.08, 4.03, and 4.62 eV Å deg^{-2}, respectively. Therefore, the Young modulus E_L and torsional rigidity c_L of the C_{60}-doped (10, 10) nanotube are observed to be lower than the corresponding values for the pure (10, 10) tube by 0.4% and 1.2%, respectively. It is also worth mentioning here that although the conventional torsional rigidity of the double-wall tube is 24% less than that of the pure tube, the value of c_L for the double-wall tube is 13.2% *more* than the corresponding value for the pure tube. The reason for this is that the conventional calculation assumes evenly distributed torsion energy, which is not correct for the double-wall tube due to the smaller deviations of the atoms of the inner shell from their equilibrium positions compared to the deviations of the atoms of the outer shell, for any fixed torsion angle.

For comparison, we also calculate E_L and c_L for the pure/C_{60}-doped (9, 9) nanotube, whose diameter, 12 Å, is less than that of the (10, 10) tube. The supercell configuration is similar to the one described above for the (10, 10) tube, except that now a (9, 9) nanotube is used[4]. We obtain E_L as 773.42 and 759.59 eV Å^{-1}, and c_L as 3.12 and 3.10 eV Å deg^{-2}, for the pure and C_{60}-doped (9, 9) nanotubes. Here, the reductions of E_L and c_L for the doped (9, 9) tube are 1.8% and 0.6%, respectively, as compared to the corresponding values for the pure tube.

Interestingly, the slight softness introduced in the nanotubes encapsulating C_{60}s indicates the higher significance of the van der Waals interaction between the C_{60} chain and the nanotube compared to that of the same interaction between separate C_{60}s within the encapsulated chain.

3.4. Poisson ratio

Using the same supercell configuration as described above for calculating the Young modulus and torsional rigidity, one can also calculate the Poisson ratio. We calculate the Poisson ratio of the C_{60}-doped (10, 10) tube at two different positions along the tube: (1) using a ring of carbon atoms between two neighbouring C_{60}s; and (2) using a ring of carbon atoms surrounding one of the C_{60}s. These two rings are then used to obtain the average radial strain u_{rr} for different values of the axial strain. The Poisson ratio σ is then obtained from $u_{rr} = -\sigma u_{zz}$.

In figure 5 we show the results obtained by deriving the optimized structures, through constrained relaxations, for different contractions/elongations of the tube. Linear fits of the results are then used to calculate the Poisson ratio for the pure tube, as well as those for the cases (1) and (2) for the doped tube. The calculated Poisson ratios turn out to be 0.320, 0.311, and 0.303 for the pure case, doped case (1), and doped case (2), respectively. These results indicate a reduction of the Poisson ratio by 2.8% and 5.3% at positions (1) and (2) of the doped tube, as compared to the pure-tube case. One may compare the pure-tube Poisson ratio calculated here with the result obtained using a force-constant model (0.280) reported by Lu [21] and that from a tight-binding calculation (0.256) carried out by Hernández *et al* [20].

[4] For calculating the elastic properties of the pure and doped (9, 9) nanotubes, the force convergence criterion is set at 0.01 eV Å^{-1} instead of 1 meV Å^{-1}. We explicitly checked that this did not have any effect on the final results reported here.

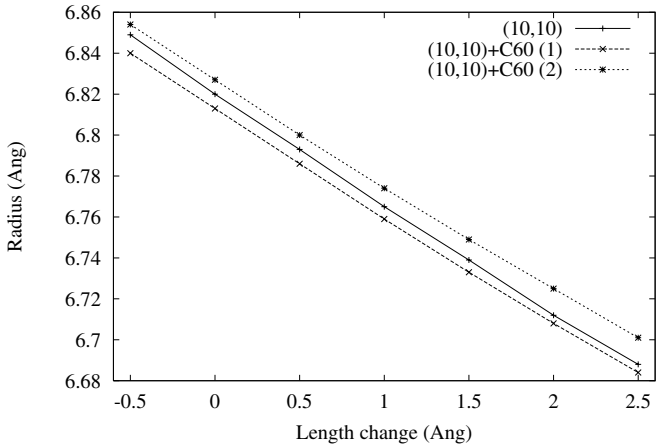

Figure 5. Average radius of a ring of carbon atoms in a (10, 10) nanotube as a function of its length change, for the pure and doped cases. (1) and (2) refer to a ring located between two neighbouring C_{60}s and a ring surrounding one of the C_{60}s respectively.

4. Conclusions

In conclusion, we observe that the preferred configuration for a C_{60} chain encapsulated by a nanotube with diameter 13.6 Å occurs when the C_{60} centres lie on the nanotube axis and a distance of ∼10–10.5 Å is maintained between the centres of the neighbouring C_{60}s. It is shown that when the electronic states of the nanotube have sufficient overlap with those of the C_{60}s, the electronic structure of the doped semiconductor tubes indicates the production of donor levels within the gap, and metallic tubes show a tendency towards metal-to-semiconductor transition. The elastic features of the doped tubes are observed to be enhanced, as indicated by a lower Young modulus and torsional rigidity compared to those of the pure nanotubes. Furthermore, the presence of the C_{60}s inside the tube causes the Poisson ratio to decrease. These changes in the electronic and mechanical properties of the fullerene-doped nanotubes can be used in practical applications. For example, a semiconductor nanotube which is partly doped with fullerene cages might act as a nano-diode, and a C_{60}-doped nanotube would be suitable for use as a scanning tunnelling microscope tip, due to its enhanced elasticity.

Acknowledgments

The authors thank S Tsuzuki and K Esfarjani for stimulating discussions and fruitful comments. The total-energy/relaxation results that we report here were obtained using the parallel density-matrix tight-binding code authored by X-P Li, D Vanderbilt, R Nunes, M Robbins, and N Modine, modified to include van der Waals interactions and the Broyden minimization scheme.

References

[1] Smith B W, Monthioux M and Luzzi D E 1998 *Nature* **396** 323
[2] Burteaux B, Claye A, Smith B W, Monthioux M, Luzzi D E and Fischer J E 1999 *Chem. Phys. Lett.* **310** 21
[3] Smith B W, Monthioux M and Luzzi D E 1999 *Chem. Phys. Lett.* **315** 31
[4] Sloan J *et al* 2000 *Chem. Phys. Lett.* **316** 191
[5] Nikolaev P, Thess A, Rinzler A G, Colbert D T and Smalley R E 1997 *Chem. Phys. Lett.* **266** 422

[6] Sánchez-Portal D, Artacho E, Soler J M, Rubio A and Ordejón P 1999 *Phys. Rev.* B **59** 12 678
[7] Xu C H, Wang C Z, Chan C T and Ho K M 1992 *J. Phys.: Condens. Matter* **4** 6047
[8] Lu J P, Li X-P and Martin R M 1992 *Phys. Rev. Lett.* **68** 1551
[9] Venkateswaran U D, Rao A M, Richter E, Menon M, Rinzler A, Smalley R E and Eklund P C 1999 *Phys. Rev.* B **59** 10 928
[10] Henrard L, Hernández E, Bernier P and Rubio A 1999 *Phys. Rev.* B **60** R8521
[11] Lu J P and Yang W 1994 *Phys. Rev.* B **49** 11 421
[12] Li X-P, Nunes R W and Vanderbilt D 1993 *Phys. Rev.* B **47** 10 891
[13] Ohno K, Esfarjani K and Kawazoe Y 1999 *Computational Materials Science from Ab Initio to Monte Carlo Methods* (Berlin: Springer)
[14] Seldin E J and Nezbeda C W 1970 *J. Appl. Phys.* **41** 3389
[15] Wang G-W, Komatsu K, Murata Y and Shiro M 1997 *Nature* **387** 583
[16] Esfarjani K, Farajian A A, Hashi Y and Kawazoe Y 1999 *Appl. Phys. Lett.* **74** 79
[17] Farajian A A, Esfarjani K and Kawazoe Y 1999 *Phys. Rev. Lett.* **82** 5084
[18] Kwon Y-K, Saito S and Tománek D 1998 *Phys. Rev.* B **58** 13 314
[19] Landau L D and Lifshitz E M 1986 *Theory of Elasticity* (Oxford: Butterworth-Heinemann)
[20] Hernández E, Goze C, Bernier P and Rubio A 1998 *Phys. Rev. Lett.* **80** 4502
[21] Lu J P 1997 *Phys. Rev. Lett.* **79** 1297
Lu J P 1997 *J. Phys. Chem. Solids* **58** 1649